Ultrafiltration of whey: membrane performance and modelling using a combined pore blocking-cake formation model

María-José Corbatón-Báguena, Silvia Álvarez-Blanco, María-Cinta Vincent-Vela*

Department of Chemical and Nuclear Engineering, Universitat Politècnica de València, C/Camino de Vera s/n 46022 Valencia, Spain

*Corresponding author: mavinve@iqn.upv.es

Tel: 96 387 93 87 (Ext.: 79387)

ABSTRACT

BACKGROUND

Ultrafiltration has been considered as a "green" technique to treat different industrial wastewaters, such as whey in the dairy industry. However, fouling is one of the major drawbacks in the industrial implementation of this process. Thus, in this work, the performance of ultrafiltration membranes was investigated in terms of permeate flux and protein rejection when treating different whey model solutions. Modelling of permeate flux was performed combining two main fouling mechanisms (complete pore blocking and cake formation) by a time-dependent pore blocking parameter.

RESULTS

Results demonstrated that high protein concentration and the presence of calcium salts in the feed solution favoured permeate flux decline. The combined model was appropriate to describe the main fouling mechanisms, with fitting accuracies higher than 0.960. Model

parameters were correlated to both calcium and protein concentration and the developed model was successfully validated with an additional fouling test.

CONCLUSION

All the membranes tested were suitable for carrying out whey protein separation, with rejection indexes greater than 99%. The combined model and the statistical correlation of model parameters with calcium and protein concentrations were useful to predict permeate flux decline when the ultrafiltration of a new whey model solution was performed.

Keywords: Ultrafiltration; whey model solutions; membrane fouling; fouling mechanisms; complete pore blocking parameter.

NOMENCLATURE

List of symbols

b	rate constant at which the parameter α grows (s^{-1})
C_{Ca}	calcium concentration in the feed solution (g/L)
J_{CF}	permeate flux of the cake formation model equation ($L/m^2 \cdot h$)
J_{CPB}	permeate flux of the complete blocking equation ($L/m^2 \cdot h$)
J_f	experimental permeate flux at the end of the fouling experiment ($L/m^2 \cdot h$)
J_i	experimental permeate flux at the beginning of the fouling experiment ($L/m^2 \cdot h$)
J_{model}	permeate flux of the combined model equation ($L/m^2 \cdot h$)
K_{CPB}	Hermia's constant of the complete pore blocking model (m^{-1})

K_{CF}	Hermia's constant of the cake formation model (s/m^2)
R^2	Regression coefficient (dimensionless)
t	ultrafiltration time (s)

Greek letters

α	time-dependent pore blocking parameter (dimensionless)
α_0	limiting value of the pore blocking parameter (dimensionless)

Abbreviations

BSA	Bovine serum albumin
FAO	Food and Agriculture Organization of the United Nations
MWCO	Molecular weight cut off
SD	Standard deviation (dimensionless)
WPC	Whey protein concentrate
WPC33	Whey protein concentrate with a protein concentration of 33 w%
WPC45	Whey protein concentrate with a protein concentration of 45 w%

INTRODUCTION

Pressure-driven membrane separation processes have become promising "green" techniques to be used in different agro-food industries, and especially in the dairy industry, because of their main advantages in comparison to the traditional concentration and separation processes (thermal evaporation, filtration or centrifugation): they require no

chemicals addition and low energy consumption to perform the separation and the operating conditions used are milder, thus allowing the organoleptic properties of the food components to be preserved.[1] From an industrial and economical point of view, the application of membrane processes in the dairy industry has an important advantage: they simultaneously allow the reduction of the pollutant character of dairy wastewaters (with high contents of biological and chemical oxygen demands) and the recovery and purification of high-added value compounds contained in such wastewaters.[2]

Dairy industry produces a wide variety of milk derived products that constitute a basic part of a healthy diet.[3] One of the most important derived products is cheese. According to the Food and Agriculture Organization of the United Nations (FAO)[4] and the European Commission[5] data, the Spanish production increased from 227000 – 387740 tonnes in 2014 to 461030 tonnes in 2016. During its manufacturing, a greenish-yellow liquid named whey is obtained in a ratio of 8-9 kg per each 1-2 kg of cheese.[6] Therefore, not only large volumes of wastewaters are produced during cheese elaboration, but also they have a high pollutant character (the chemical oxygen demand value of this wastewaters can reach 100 g O_2/L).[7] However, whey components have nutritional, biological and functional properties of interest for other industrial fields, such as the pharmaceutical industry or the fine chemical one: lactic acid (used as food preservative), lactose (part of health care supplements due to its agglomerating properties and low glycemic index), fat (used in bakery products for its creaming properties), vitamins A, D or E (part of cosmetics composition) and whey proteins (used in cosmetics, infant formulae, food products and health care supplements for their emulsifying, encapsulating, gelling, foaming, immunological, antioxidant and antimicrobial properties).[8] Due to the outstanding properties and benefits of the protein fraction of whey, the separation and concentration of

such proteins is of great interest. Thus, the commercial value of whey protein concentrates (WPC) is up to 40 times greater than that of whey in powder form.[6]

To produce whey protein concentrates, ultrafiltration membranes are widely used.[9-12] This membranes are able to retain proteins, while lactose and mineral salts transfer to the permeate stream. However, during the filtration process, proteins may deposit on the membranes surface as well as inside their pores.[13] This phenomenon, named membrane fouling, results in a decrease in the global process productivity since permeate flux diminishes over time. Therefore, membrane fouling is a drawback of a great technical and economical importance. Thus, significant efforts have been made to predict membrane fouling and optimize the operating conditions used during the ultrafiltration process to minimize this phenomenon. For instance, mathematical models have been fitted to the experimental data to describe the fouling mechanisms governing the process[14-19]. Yuan et al. studied the membrane fouling during the microfiltration of humic acid by the combination of two fouling mechanisms: pore blockage and cake filtration. Their results demonstrated that the large humic acid aggregates are the responsible for the pore blockage, while the cake is formed onto these pores previously blocked[20]. Previously to Yuan et al., Ho and Zydney developed a mathematical model that accounts for the pore blockage (at the beginning of the filtration process) followed by the formation of a cake. With only one mathematical equation they could explain two fouling phenomena taking place during the microfiltration of BSA solutions[14]. In the same way, Mondal and De sequentially combined complete pore blocking and cake formation mechanisms in the same mathematical model. For that purpose, they divided the entire filtration time in two parts: the first one corresponding to the complete pore blocking equation and the second one where the two mechanisms are combined together.[21]

Among the different models tested, semi-empirical models are the most suitable due to the combination of high fitting accuracy and the ability to describe fouling mechanisms using parameters with physical meaning.[22,23] According to the literature, the classical models developed by Hermia[24] and their adaptations to crossflow ultrafiltration[25,26] are the most often used by different authors and feed solutions. As examples, Salahi et al. investigated the fitting accuracy of the four classical models (complete, standard and intermediate pore blocking and cake formation) to the experimental data obtained in the ultrafiltration of oily wastewaters using a polymeric membrane, achieving values of R^2 from 0.985 to 0.999.[22] Said et al. fitted the classical Hermia's models to the ultrafiltration of a palm oil mill effluent under different operating conditions. They obtained values of R^2 of 0.981 as the best fitting results.[27] In addition, other authors studied the combination of two of these mechanisms in the same mathematical equation. For instance, De la Casa et al. studied different combinations of the Hermia's dead-end complete pore blocking, cake formation and standard pore blocking equations to simulate the permeate flux decline during the microfiltration of bovine serum albumin (BSA).[28]

Therefore, as pore blocking and cake formation mechanisms are the predominant ones in the ultrafiltration of protein based solutions[14], the main objective and novelty of this work was to describe the temporal evolution of a time-dependent pore blocking parameter (α) by means of its limiting value (α_0) and the rate constant at which membrane pores were completely blocked (b). This time-dependent parameter (α) was used to combine, in the same mathematical equation, two fouling mechanisms: complete pore blocking and cake formation. Equations for each individual mechanism were taken from the Hermia's models adapted to crossflow ultrafiltration. Whey model solutions that contained BSA (10 g/L),

BSA with $CaCl_2$ (1.65 g/L) and WPC with a protein content of 45 % (WPC45) at three different concentrations (22.2, 33.3 and 44.4 g/L) were used as feed solutions and, as another novel aspect, model parameters were correlated to the feed solution composition (calcium and protein concentrations). Using these correlations, the developed model was validated with a different whey model solution (WPC with a 33 % protein content, WPC33).

MODEL DEVELOPMENT

Hermia developed four classical models explaining the membrane fouling mechanisms caused by solute molecules. Briefly, solute molecules of a similar size than membrane pores can deposit onto the membrane and completely clog the pores (complete blocking) or partially block them (intermediate blocking). When these molecules are smaller than membrane pores, they can be adsorbed on the pore walls (standard blocking); whereas if these molecules are much larger than membrane pores, they accumulate onto the membrane and form a cake (cake formation).[24] These models were developed for dead-end filtration. However, they have also been adapted to crossflow ultrafiltration.[25]

Several authors[14,28] reported that, during the first minutes of operation, a pore blocking mechanism is the main responsible for the sharp permeate flux decline; while the formation of a cake by the accumulation of solute molecules is the mechanism governing the long term flux decline until the steady-state is achieved. Therefore, the mathematical model used in this work considered both fouling mechanisms. The model combined the general equations for the Hermia's complete pore blocking and cake formation models adapted to crossflow ultrafiltration to simulate with higher accuracy the permeate flux

decline, since crossflow ultrafiltration was the operating mode selected (see Section 3).[26] This constitutes a novelty of this work with regard to previous works, where a similar combination using the classical dead-end filtration equations developed by Hermia was reported.[28] Besides, similar combinations of two fouling mechanisms were fitted to different solutions systems (residual brines from table olive storage wastewaters[29] and enzymatic solutions[30]), but none of them considered the temporal variation of the pore blocking parameter. In addition, both mechanisms (complete blocking and cake formation) were combined through a complete pore blocking parameter (α), which represents the fraction of completely blocked membrane pores, i.e. the membrane pores that were clogged by a solute molecule with regard to the total membrane pores. As explained before, these pores are gradually blocked over the ultrafiltration time and thus, a temporal evolution of the parameter α was included in the general model equation. This evolution is a novel aspect of this work, since to the best of our knowledge, most of the works on mathematical modelling of ultrafiltration processes do not account for the temporal variation of the model parameters.[17,22,28,31] According to other authors that use exponential equations to express the upward evolution of different parameters (such as the hydraulic resistance due to solute adsorption onto the membrane or the limiting flux),[32,33] in this work the parameter α was also correlated to the filtration time through a limiting value, α_0 , and a growth rate constant, b (see Eq. 3).

The following mathematical equations show the Hermia's models adapted to crossflow ultrafiltration for the complete blocking (Eq. 1) and cake formation mechanisms (Eq. 2),[26] as well as the general equation for the combined model developed in this work (Eq. 3):

$$J_{CPB} = J_f + (J_i - J_f)exp(-K_{CPB} J_i t) \qquad \text{Eq. 1}$$

$$t = \frac{1}{K_{CF} J_f} ln\left[\left(\frac{J_{CF}}{J_i}\frac{J_i - J_f}{J_{CF} - J_f}\right) - J_f\left(\frac{1}{J_{CF}} - \frac{1}{J_i}\right)\right] \quad \text{Eq. 2}$$

$$J_{model} = \alpha \cdot J_{CPB} + [1-\alpha] J_{CF} \text{ with } \alpha = \alpha_0 (1 - exp(-b \cdot t)) \quad \text{Eq. 3}$$

where J_i is the experimental permeate flux at the beginning of the ultrafiltration test, J_f is the experimental permeate flux at the end of the ultrafiltration experiment, J_{model} is the permeate flux calculated by the combined model equation, J_{CPB} is the permeate flux calculated by the complete pore blocking equation, K_{CPB} is the Hermia's constant of the complete pore blocking model, J_{CF} is the permeate flux calculated by the cake formation model equation, K_{CF} is the Hermia's constant of the cake formation model, α is the pore blocking parameter, α_0 is the limiting value of the pore blocking parameter, b is the rate constant at which the parameter α grows and t is the filtration time.

EXPERIMENTAL

Experimental set-up

A conventional crossflow ultrafiltration plant at laboratory scale (VF-S11 model, Orelis, France) was used for the ultrafiltration tests. The plant was equipped with two different membrane modules, according to the membrane used in each test: a monotubular, stainless-steel one for the ceramic membrane and a Rayflow one (Orelis, France) for the polymeric membranes. Crossflow velocity and transmembrane pressure were regulated by a frequency variator connected to a volumetric pump and two manometers placed at the

inlet and outlet streams of the membrane module, respectively. Permeate flux was gravimetrically measured by means of a scale with an accuracy of ±0.001 g. Temperature of all ultrafiltration tests was kept constant at 25 ± 1 ºC.

Membranes

Experiments were performed with three ultrafiltration membranes of different MWCO and material:[34]

- A flat-sheet 5 kDa membrane made of polyethersulfone (UP005, Microdyn Nadir, Germany) with an effective area of 100 cm^2 and a Root Mean Square surface roughness of 0.487 nm.
- A monotubular 15 kDa membrane made of ZrO_2-TiO_2 (Inside-Céram, TAMI Industries, France). It has a Root Mean Square surface roughness of 17.900 nm, 35.5 cm^2 of effective area, 20 cm in length and 0.6 and 1 cm of internal and external diameters, respectively.
- A flat-sheet 30 kDa membrane made of permanently hydrophilic polyethersulfone (UH030, Microdyn Nadir, Germany) with an effective area of 100 cm^2 and a Root Mean Square surface roughness of 1.657 nm.

Chemicals and analytical methods

Different whey model solutions were used as feed for the ultrafiltration experiments:

- BSA (A3733, Sigma-Aldrich, Germany) solutions at a concentration of 10 g/L.
- BSA and $CaCl_2$ (Panreac, Spain) solutions with a protein concentration of 10 g/L and a calcium concentration of 0.6 g/L.

- Solutions prepared from a WPC with a total protein content of 45 w% (WPC45, Industrias Lácteas Asturianas, Spain). The composition of the WPC45 is shown in Table 1. Three different solutions were prepared with different concentrations of WPC (22.22, 33.33 and 44.44 g/L). These solutions had protein concentrations of 9.05, 13.58 and 18.11 g/L, respectively and calcium concentrations of 0.17, 0.26 and 0.35 g/L, respectively.

Additionally, an aqueous solution of a commercial WPC with a total protein content of 33 w% (WPC33, Industrias Lácteas Asturianas, Spain) at a concentration of 30.3 g/L was ultrafiltered with the 30 kDa membrane to validate the developed model. The composition of this powdered WPC is shown in Table 1. The solution had a protein concentration of 8.35 g/L and a calcium concentration of 0.31 g/L. All these feed solutions were prepared by dissolving in deionized water the protein-based powder until reaching the desired concentration and with no pH adjustment (pH values ranging from 5.9-6.5). The analytical procedures used to determine the concentration of each component in the WPC are described in a previous work.[35]

To determine the protein concentration in feed, retentate and permeate samples the Bradford colorimetric method was used.[36] For this purpose, the Bradford reagent (Sigma Aldrich, Germany) was added to the samples and their absorbance was measured by means of a UV-visible spectrophotometer (Hewlett-Packard 8453) at 595 nm.

Experimental procedure

Ultrafiltration experiments were performed in total recirculation mode at a crossflow velocity of 2 m/s, a transmembrane pressure of 2 bar and at 25 ºC. The operating conditions were selected according to previous studies about protein ultrafiltration.[37] During 2 hours, permeate flux was monitored to evaluate the performance of each membrane and fit the mathematical models described in Section 2 (Eqs. 1-3). Simultaneously, permeate samples of 10 mL were collected to measure protein concentration. Knowing the values of protein concentration in the feed solution (C_{feed}) and in the permeate stream ($C_{permeate}$), the percentage of protein rejection can be calculated by Eq. 4:

$$\text{Rejection } (\%) = \left(1 - \frac{C_{permeate}}{C_{feed}}\right) \cdot 100 \qquad \text{Eq. 4}$$

Model fitting, validation and statistical analyses

Once the permeate flux data was obtained for all the feed solutions and membranes tested, a least-squares minimization curve-fitting method based on the Levenberg-Marquadt algorithm was used (by means of the "Genfit" function of the MathCad® software). For each case of study, the regression coefficient and the standard deviation were calculated to express the accuracy of the model predictions. The fitting procedure consisted in the following steps:

- First, Hermia's equations of the complete blocking and cake formation models were fitted to the experimental data (Eqs. 1 and 2). In this way, the values of the parameters K_{CPB} and K_{CF} for the abovementioned models, respectively, were obtained.

- Once the values of K_{CPB} and K_{CF} were known and using the experimental values of initial (J_i) and final (J_f) permeate fluxes, the combined model was fitted to the experimental data (Eq. 3). Thus, the values of α_0 and b and the temporal evolution of the pore blocking parameter α were determined for each experimental condition.

To generalise the values of the model parameters obtained, several multiple regression analyses were carried out with the Statgraphics Centurion XVI software to correlate each model parameter (K_{CPB}, K_{CF}, α_0 and b) to the feed solution characteristics (calcium and protein concentrations). Once these equations were obtained, they were substituted in the general combined model equation (Eq. 3).

Finally, the validation of the proposed model was performed with the results obtained in a new ultrafiltration test that was not used to predict model parameters. By substituting the values of calcium and protein concentrations in the multiple regression equations described above, the permeate flux decline predicted by the combined model was obtained and then, it was compared to the experimental data.

RESULTS AND DISCUSSION

Ultrafiltration of whey model solutions

Fig. 1 shows the evolution of permeate flux over time for the three membranes used (5, 15 and 30 kDa) and the different feed solutions ultrafiltered (BSA, BSA+$CaCl_2$ and the three WPC45 w% solutions). In the figure, the combined model predictions obtained with the Levenberg-Marquadt algorithm are represented in solid lines and the experimental data

collected are depicted with symbols. The experimental variation of permeate flux with time can be explained, according to the literature commented in the introduction section, as a two-phase process: the first one is a rapid flux decline during few minutes after the beginning of the ultrafiltration (at time scales lower than 15 minutes for all the membranes and feed solutions tested), while the second phase consists of a more slow decrease until achieving an almost constant value.[14,38] This performance is related to membrane fouling. The rapid initial flux decline is attributed to a pore blocking mechanism while the slow decrease of flux corresponds to the formation of a cake onto the membrane surface.[39]

The experimental permeate flux depicted in Fig. 1 shows important differences among the whey model solutions and membranes tested. On the one hand, regarding the effect of protein concentration, the greater it was in the feed solution, the lower the permeate flux measured at the end of the ultrafiltration process and the permeate flux decline between the beginning and the end of the process were for a fixed membrane. For instance, comparing the values of permeate flux decline during the ultrafiltration of WPC45 solutions at two different protein concentrations (22.2 and 44.4 g/L) for the 5, 15 and 30 kDa membranes, the permeate flux decline was greater for the 44.4 g/L WPC45 solution (and 43.08, 50.52 and 28.51 %, respectively). This fact confirmed that membrane fouling was more severe when higher amount of proteins were able to reach the membrane surface and deposit on it, due to the higher aggregation effect.[40] In addition, it can be observed that the 15 kDa membrane was the one with the greatest permeate flux decline when protein concentration increased from 22.2 g/L WPC solution to the 44.4 g/L one. Some authors reported that flat-sheet membranes allocated in plate-and-frame modules are more sensitive to fouling than the tubular configuration, in which the concentration polarization and membrane fouling phenomena can be controlled[41]. This is due to the fact that tubular configurations allow the

operation at higher flow velocity and thus high shear[42]. Taking this information into account, the 15 kDa membrane should not show the greatest permeate flux decline in comparison to the other two flat-sheet membranes tested. But in this case this more severe membrane fouling that the tubular ceramic membrane shows is not mainly due to its configuration, but to its rougher membrane surface. As other authors reported, rougher surfaces ease the entrapment of solute molecules (as proteins in this work) and thus, a thicker cake layer can be formed on the membrane surface.[43,44]

On the other hand, regarding the effect of salt concentration, the decline in the permeate flux measured increased from the ultrafiltration of BSA to that of the BSA with $CaCl_2$ solution for the three membranes used. According to the experimental data, the steady-state value of the permeate flux declined from 46.84 to 22.92 $L/m^2 \cdot h$, from 48.96 a 29.53 $L/m^2 \cdot h$ and from 89.14 to 61.16 $L/m^2 \cdot h$ for the 5, 15 and 30 kDa membranes. These data show that permeate flux decline, and thus membrane fouling, was more severe when a combination of salts and proteins was used as feed solution. Considering previous studies about the filtration of protein-salt solutions, Ang et al. reported that calcium can form bridges between organic foulant chains after specifically bound to the carboxylic functional groups present in such organic foulants, as in the case of whey proteins. This fact accelerates fouling by charged organic molecules, causing a crosslinked fouling layer onto the membrane surface and resulting in a severe membrane fouling.[45]

Taking into account the composition of the feed solutions, proteins are the mainly retained compounds and the major responsible for membrane fouling.[13] At this regard, Table 2 shows protein concentration in the feed for the different feed solutions tested as well as the rejection of proteins determined for each membrane. As it can be observed, rejection

percentages were greater than 99 % for all the membranes, which can be explained by the larger size of solute molecules compared to that of the membrane pores. According to the manufacturer, BSA molecules have a size of 66-67 kDa and, as other authors reported, the commercial WPC 45 w% used contains small proteins (α-lactalbumin of 14 kDa and β-lactoglobulin of 18 kDa) with tendency to form dimers or trimers at the pH values used in this work.[46,47] Besides, the presence of different salts in the feed solutions (as calcium salts) enhances the agglomeration of proteins, increasing their effective size and favouring their retention by the membrane.[48,49] Therefore, as high rejection values were obtained in all cases, the suitability of these membranes to perform the separation of whey proteins from whey model solutions can be confirmed.

Mathematical modelling

Once the general equation for the combined model was fitted to the experimental data obtained with all the whey model solutions and membranes tested, the values of the model parameters (Table 3) and the fitting accuracy in terms of the regression coefficient and standard deviation (Table 4) were determined. As it can be observed in Table 4, the fitting accuracy of the combined model is higher than that of the individual complete blocking and cake formation ones in all cases.[34] The only exception was the 30 kDa membrane fouled with WPC 45 w% at 33.3 g/L, although the difference between the combined model (R^2 of 0.960 and SD of 0.016) and the complete pore blocking (R^2 of 0.962 and SD of 0.015) was not statistically significant. Therefore, it can be concluded that the combination of complete pore blocking and cake formation fouling mechanisms through a time-dependent pore blocking parameter is appropriate to predict the permeate flux decline of ultrafiltration membranes fouled with whey model solutions.

On the other hand, Table 3 shows the values of the model parameters K_{CPB}, K_{CF}, α_0 and b for each experimental condition tested. Regarding the effect of protein concentration, it is important to note that the values of K_{CPB}, K_{CF} and α_0 increased for a fixed membrane when the feed solution became more concentrated (from 22.2 g/L WPC45 to 44.4 g/L WPC45 solution).[26] As protein concentration in the feed solution increased, protein aggregation increased as well and therefore, more severe membrane fouling due to a thicker layer on membrane surface occurs.[50] On the other hand, when salts were combined with proteins in the feed solution (i.e. comparing the results obtained for BSA and BSA with $CaCl_2$ solutions), the values of model parameters K_{CPB}, K_{CF} and α_0 also increased for a fixed membrane. As it was explained before, the presence of calcium salts in the feed solution enhances the formation of bridges between protein molecules and thus, the fouling layer formed onto the membrane surface may be thicker.[45]

Comparing the values of K_{CPB} and K_{CF} for a certain feed solution and different membranes, the general trend for both parameters is to decrease when the MWCO increased from 5 to 30 kDa. This may be due to the fact that the 5 kDa polyethersulfone membrane is more hydrophobic than the other two membranes (made of metal oxides and permanently hydrophilic polyethersulfone, respectively). Therefore, protein molecules were preferentially deposited on the hydrophobic 5 kDa membrane surface, blocking its pores entrance and forming a thicker cake on it; while the hydrophilic 30 kDa membrane was the one showing the lowest membrane fouling. As other authors reported, the hydrophobic residues of organic macromolecules tend to preferentially adsorb onto hydrophobic surfaces[51] and also, the packing of these molecules in a cake on the hydrophobic surface is denser than in the case of a hydrophilic one. For instance, Igbinigun et al. studied the

performance of several ultrafiltration membranes with different hydrophilic character and fouled by an organic compound (humic acid). They reported that the hydrophobic groups of the foulant molecules interacted with the hydrophobic surfaces of the commercial polyethersulfone membrane, resulting in a higher rate of fouling and permeate flux decline. On the other hand, these authors also observed that the attachment of foulant molecules to the membrane surface was diminished when hydrophilic membranes with less rougher surfaces (as occurs with the 30 kDa membrane in this work in comparison with the 15 kDa membrane) were used.[52] In addition, Rahimpour and Madaeni investigated membrane performance during the crossflow ultrafiltration of non-skim milk. They observed that hydrophilic membranes presented low surface fouling by milk proteins and fat, because the loose interactions between hydrophobic foulants and hydrophilic surfaces favoured the removal of foulants by the crossflow shear stress.[53] Besides the effect of hydrophilicity/hydrophobicity, the greatest values of model parameters observed for the 5 kDa membrane may be due to the fact that flat-sheet membranes are more prone to fouling that the tubular ones. Some authors reported that flat-sheet membranes allocated in plate-and-frame modules are more sensitive to fouling than the tubular configuration, in which the concentration polarization and membrane fouling phenomena can be controlled[41]. This is due to the fact that tubular configurations allow the operation at higher flow velocity and thus high shear[42]. Additionally to its different configuration, the lowest pore size that the 5 kDa membrane has in comparison to the other membranes tested in this work may result in a tighter and thicker cake layer formed onto its surface.

As regards the membrane pore size, it is well known that due to the sieving effect that dominates ultrafiltration processes, as the membrane pore size increased there is more space available for the foulant molecules to penetrate inside the porous structure and

blocked them, thus increasing irreversible membrane fouling[54]. This means that, in the case of our study, the 30 kDa membrane should show the greatest values of the model parameters, as well as the highest decline in permeate flux at the end of the filtration process. However, the trend observed for the 30 kDa membrane is exactly the opposite, being the membrane tested with the lowest values of K_{CPB} and K_{CF}. Therefore, the experimental pattern reported for the three membranes tested in this work could not be explained except by the hydrophilic character of the 30 kDa membrane in comparison with the 5 and 15 kDa membranes. In addition, although tubular configurations allow high flow velocities and high shears (which make them more resistant to fouling) in comparison to flat-sheet configurations, the higher surface roughness of ceramic membranes than polymeric ones is a crucial drawback when fouling phenomena appears. Surface roughness is an influential parameter in membrane fouling. Rougher surfaces favour the deposition and entrapment of solute molecules onto the membrane structure, thus being smooth surfaces more difficult to be fouled. For this reason, the surface properties such as high hydrophilic character and low roughness are dominant factors to reduce membrane fouling[55].

Regarding the values of the parameter b, no clear pattern can be inferred from the fitting data obtained, since similar values were obtained for the different membranes and whey protein solutions tested. However, the parameter b should be very similar in all the experiments due to the fact that all molecules have a higher size than the membrane pore size. Other authors have studied its behaviour and could not relate the values of parameter b with the experimental conditions tested[32]. Therefore, an average value of this parameter for each membrane used was calculated in order to validate the combined model

(explained in Section 4.3): 0.180, 0.162 and 0.259 s^{-1} for the 5, 15 and 30 kDa membranes, respectively.

Statistical analyses

Once the values of α_0, K_{CPB} and K_{CF} were obtained for all the feed solutions tested, statistical analyses were performed to identify which operating parameters (calcium concentration, protein concentration or their combinations) had statistically significant influence on the model parameters. In these analyses, only the operating parameters or combination of them whose p-value was higher than 0.05 (corresponding to a confidence level of 95 %) were considered in the final multiple regression equations that correlate the model parameters to the calcium concentration (C_{Ca}) and the protein concentration (C_{prot}). The general expressions for these equations are shown in Table 5 (Eqs. 5-13). As it can be observed, only the second-order combination of operating parameters (C_{Ca}^2, C_{prot}^2 and $C_{Ca} \cdot C_{prot}$) have a statistically significant influence on the model parameters. Among the three statistically significant parameters, the one with the greatest influence is the combination of both calcium and protein concentrations $C_{Ca} \cdot C_{prot}$. As it can be inferred from Table 5, Eqs. 5-13 show a parabolic pattern for all the model parameters with the calcium concentration. At low calcium concentrations, the values of the model parameters increased as this concentration increased. However, at the highest calcium concentration tested, no further increase in these parameters was achieved. This may be due to the fact that, at low protein concentrations, there are not enough reaction sites available to crosslink to the excess of calcium ions. As the membranes used were ultrafiltration ones, the calcium that did not react with the protein chains cannot be retained by these membranes and thus it can pass through the permeate stream.

To better observe the pattern of the multiple regression correlations shown in Table 5, the surface contour plots for each model parameter as a function of calcium and protein concentrations can be depicted. As an example, Fig. 2 shows the contour plots for the three model parameters α_0, K_{CPB} and K_{CF} obtained with the 30 kDa membrane. White colour corresponded to the combination of operating conditions that led to the lowest value of model parameters, while dark colours represented the operating conditions for which membrane fouling was more severe and thus, the parameters had a larger value. As it was explained before, the higher the combination of both calcium and protein concentration in the feed solution was, the more severe the membrane fouling was and thus, the greater values the model parameters were. As it was previously highlighted, all the model parameters had the same general correlation to the operating variables (C_{Ca} and C_{prot}) for the 30 kDa membrane. Thus, the three contour plots depicted in Figs. 2a-c show similar tendencies with both calcium and protein concentrations. Regarding the evolution of the model parameters related to the complete pore blocking mechanism (K_{CPB} and α_0), Figs. 2a and 2b show that at high protein concentration, a small increase in calcium concentration resulted in a great increase in both parameters. This tendency can also be observed in Fig. 2c for the results of the cake formation parameter K_{CF}. In this case, the greatest value of K_{CF} was obtained at calcium concentrations of 0.50-0.60 g/L and protein concentrations of 18-20 g/L, respectively, which were the greatest concentrations considered. These patterns can be due to the fact that a thicker cake layer was preferentially formed onto the membrane surface when feed solutions contained high calcium and protein concentrations, favouring protein aggregation and accumulation on the membrane.[40]

Validation of the model

In this work, an additional ultrafiltration experiment was performed with the 30 kDa membrane. The feed solution was prepared from a WPC with different protein concentration (33 w% in dry basis, WPC33). The composition of the WPC33 is shown in Table 1. The concentration of the WPC was 30.3 g/L. The transmembrane pressure (2 bar), crossflow velocity (2 m/s) and temperature (25 ºC) remained unchanged. In this way, it could be confirmed if the combined model predictions were accurate when a different whey model solution was used.[56-59]

Fig. 3 shows the temporal evolution of permeate flux for the 30 kDa membrane and the WPC33 model solution. The experimental data obtained during the ultrafiltration process was depicted in symbols, while the permeate flux predicted by the combined model was represented by solid lines. In order to obtain the values of the model parameters, the concentration of calcium (0.31 g/L) and protein (8.35 g/L) were included in Eqs. 11-13 (see Table 5). Since the values of the parameter b could not be correlated to the calcium and protein concentrations, its average value for the 30 kDa membranes was used (0.259 s^{-1}). The parameters α_0, K_{CPB} and K_{CF} had values of 0.774, 42.034 m^{-1} and $4.283 \cdot 10^6$ s/m^2, respectively. At these experimental conditions a fitting accuracy of 0.940 in terms of regression coefficient and a standard deviation of 0.037 were achieved. In this case, the 30.3 g/L WPC33 solution contains a protein concentration similar to that of the 22.2 g/L WPC45 solution (8.35 and 9.05 g/L, respectively) and a calcium concentration similar to that of the 44.4 g/L WPC45 solution (0.31 and 0.35 g/L, respectively). Therefore, the values of the model parameters obtained for the 30 kDa membranes and the WPC33 solution were higher than those obtained for the same membrane and the 22.2 g/L WPC45

solution (see Table 3), due to the higher calcium concentration present in the WPC33 than in the WPC45 solution.

CONCLUSIONS

- The 5kDa flat-sheet polyethersulfone membrane, the 15 kDa monotubular ceramic membrane and the 30 kDa flat-sheet permanently hydrophilic polyethersulfone membrane were suitable to perform the separation of whey proteins from whey model solutions since rejection percentages greater than 99 % were obtained in all the conditions tested.

- The combined model proposed in this work, which is based on the Hermia's crossflow complete blocking and cake formation mechanisms combined through a time-dependent pore blocking parameter (α), fitted the experimental data with high accuracy in terms of the regression coefficient and standard deviation. For that reason, it can be concluded that this combined model is appropriate to describe the temporal evolution of permeate flux when ultrafiltering the whey model solutions tested at 2 bar and 2 m/s with membranes from 5 to 30 kDa.

- Regarding the values of the model parameters, α_0, K_{CPB} and K_{CF}, they increased when the composition of the feed solution became more complex for a certain membrane (i.e., salts were added and high protein concentrations were considered). This was due to the more severe fouling that the membranes experienced in such conditions.

- Comparing the model parameters for the three membranes tested, it can be concluded that the hydrophilic nature of the 30 kDa membrane favoured its lower fouling and thus, lower values of the model parameters K_{CF} and K_{CPB} were obtained for this membrane. In addition, the general trend of the model parameters was to decrease from the 5 kDa to the 30 kDa membranes, due to an increase in membrane hydrophilicity. Besides the effect of hydrophilicity, the lowest pore size that the 5 kDa membrane has in comparison to the other membranes tested in this work may result in a tighter and thicker cake layer formed onto its surface.

- Multiple regression analyses were conducted with all the membranes and feed solutions considered to correlate the fitting values of the model parameters α_0, K_{CPB} and K_{CF} to the calcium and protein concentrations of the whey model solutions used. In all the cases, multiple regression equations fitted with high accuracy the values of the parameters (with regression coefficients ranging from 0.984 to 0.999).

- Good fitting accuracy was achieved between the combined model estimations obtained with the 30 kDa membrane and a 30.3 g/L WPC33 solution (not used for the model development). Thus, it was confirmed that the combined model was appropriate to predict permeate flux decline in whey model solutions ultrafiltration.

ACKNOWLEDGEMENTS

This work was supported by the Spanish Ministry of Science and Innovation (project CTM2010-20186).

REFERENCES

1 Daufin G, Escudier JP, Carrère H, Bérot S, Fillaudeau L and Decloux M, Recent and emerging applications of membrane processes in the food and dairy industry. *Trans IChemE* **79**: 89-102 (2001).

2 Castro-Muñoz R, Yáñez-Fernández J and Fíla V, Phenolic compounds recovered from agro-food by-products using membrane technologies: An overview. *Food Chem* **213**: 753-762 (2016).

3 Palmieri N, Forleo MB and Salimei S, Environmental impacts of a dairy cheese chain including whey feeding: An Italian case study. *J Cleaner Prod* **140**: 881-889 (2017).

4. Food and Agriculture Organization of the United Nations statistics. http://www.fao.org/faostat/en/#data/QP [accessed 25.11.2016].

5 European Commission statistics. http://ec.europa.eu/eurostat/tgm/table.do?tab=table&plugin=1&language=en&pcode=tag00040 [accessed 25.11.2016].

6 Baldasso C, Barros TC and Tessaro IC, Concentration and purification of whey proteins by ultrafiltration. *Desalination* **278**: 381-386 (2011).

7 Yorgun MS, Balcioglu IA and Saygin IO, Performance comparison of ultrafiltration, nanofiltration and reverse osmosis on whey treatment. *Desalination* **229**: 204–216 (2008).

8 Ramchandran L and Vasiljevic T, Chapter 9: Whey Processing, in *Membrane Processing: Dairy and Beverage Applications*, ed Tamime AY. Blackwell Publishing, United Kingdom, pp 193-207 (2013).

9 Metsämuuronen S and Nyström M, Enrichment of α-lactalbumin from diluted whey with polymeric ultrafiltration membranes. *J Membr Sci* **337**: 248-256 (2009).

10 Arunkumar A and Etzel MR, Fractionation of α-lactalbumin and β-lactoglobulin from bovine milk serum using staged, positively charged, tangential flow ultrafiltration membranes. *J Membr Sci* **454**: 488-495 (2014).

11 Brião VB and Tavares CRG, Pore blocking mechanism for the recovery of milk solids from dairy wastewater by ultrafiltration. *Braz J Chem Eng* **29**: 393–407 (2012).

12 Pal P and Nayak J, Development and analysis of a sustainable technology in manufacturing acetic acid and whey protein from waste cheese whey. *J Cleaner Prod* **112**: 59-70 (2016).

13 Argüello MA, Álvarez S, Riera FA and Álvarez R, Enzymatic cleaning of inorganic ultrafiltration membranes used for whey protein fractionation. *J Membr Sci* **216**: 121-134 (2003).

14 Ho C-C, Zydney AL, A combined pore blockage and cake filtration model for protein fouling during microfiltration. *J Colloid Interface Sci* **232**: 389-399 (2000).

15 Choi S-W, Yoon J-Y, Haam S, Jung J-K, Kim J-H and Kim W-S, Modeling of the permeate flux during microfiltration of BSA-adsorbed microspheres in a stirred cell. *J Colloid Interface Sci* **228**: 270-278 (2000).

16 Chen H and Kim AS, Prediction of permeate flux decline in crossflow membrane filtration of colloidal suspension: a radial basis function neural network approach. *Desalination* **192**: 415-428 (2006).

17 Bolton G, LaCasse D and Kuriyel R, Combined models of membrane fouling: development and application to microfiltration and ultrafiltration of biological fluids. *J Membr Sci* **277**: 75-84 (2006).

18 Mondal S and De S, A fouling model for steady state crossflow membrane filtration considering sequential intermediate pore blocking and cake formation. *Sep Purif Technol* **75**: 222-228 (2010).

19 Wang C, Li Q, Tang H, Yan D, Zhou W, Xing J and Wan Y, Membrane fouling mechanism in ultrafiltration of succinic acid fermentation broth. *Biores Technol* **116**: 366–371 (2012).

20 Yuan W, Kocic A, Zydney AL, Analysis of humic acid fouling during microfiltration using a pore blockage-cake filtration model. *J Membr Sci* **198**: 51-62 (2002).

21 Mondal S, Sirshendu D, Generalized criteria for identification of fouling mechanism under steady state membrane filtration. *J Membr Sci* **344**: 6-13 (2009).

22 Salahi A, Abbasi M and Mohammadi T, Permeate flux decline during UF of oily wastewater: experimental and modelling. *Desalination* **251**: 153–160 (2010).

23 Mah S-K, Chuah C-K, Lee WPC and Cahi S-P, Ultrafiltration of palm oil-oleic acid-glycerin solutions: fouling mechanism identification, fouling mechanism analysis and membrane characterizations. *Sep Purif Technol* **98**: 419-431 (2012).

24 Hermia J, Constant pressure blocking filtration laws — application to power-law non-Newtonian fluids. *Trans IChemE* **60**: 183–187 (1982).

25 Field RW, Wu D, Howell JA and Gupta BB, Critical flux concept for microfiltration fouling. *J Membr Sci* **100**: 259–272 (1995).

26 Vincent Vela MC, Álvarez Blanco S, Lora García J and Bergatiños Rodríguez E, Analysis of membrane pore blocking models adapted to crossflow ultrafiltration in the ultrafiltration of PEG. *Chem Eng J* **149**: 232–241 (2009).

27 Said M, Ahmad A, Mohammad AW, Nor MTM and Abdullah SRS, Blocking mechanism of PES membrane during ultrafiltration of POME. *J Ind Eng Chem* **21**: 182-188 (2015).

28 De la Casa EJ, Guadix A, Ibáñez R, Camacho F and Guadix EM, A combined fouling model to describe the influence of the electrostatic environment on the cross-flow microfiltration of BSA. *J Membr Sci* **318**: 247–254 (2008).

29 Carbonell-Alcaina C, Corbatón-Báguena MJ, Álvarez-Blanco S, Bes-Piá MA, Mendoza-Roca JA, Pastor-Alcañiz L, Determination of fouling mechanisms in polymeric ultrafiltration membranes using residual brines from table olive storage wastewaters as feed. *J. Food Eng.* **187**: 14-23 (2016).

30 Corbatón-Báguena MJ, Gugliuzza A, Cassano A, Mazzei R, Giorno L, Destabilization and removal of immobilized enzymes adsorbed onto polyethersulfone ultrafiltration membranes by salt solutions. *J. Membr. Sci.* **486**: 207-214 (2015).

31 De Barros STD, Andrade CMG, Mendes ES and Peres L, Study of fouling mechanism in pineapple juice clarification by ultrafiltration. *J Membr Sci* **215**: 213-224 (2003).

32 Carrère H, Blaszkow F and Roux de Balmann H, Modelling the clarification of lactic acid fermentation broths by cross-flow microfiltration. *J Membr Sci* **186**: 219-230 (2001).

33 Astudillo-Castro C, Limiting flux and critical transmembrane pressure determination using an exponential model: the effect of concentration factor, temperature, and cross-flow velocity during casein micelle concentration by microfiltration. *Ind Eng Chem Res* **54**: 414-425 (2015).

34 Corbatón-Báguena M-J, Álvarez-Blanco S and Vincent-Vela M-C, Fouling mechanisms of ultrafiltration membranes fouled with whey model solutions. *Desalination* **360**: 87-96 (2015).

35 Corbatón-Báguena M-J, Álvarez-Blanco S, Vincent-Vela M-C and Lora-García J, Utilization of NaCl solutions to clean ultrafiltration membranes fouled by whey protein concentrates. *Sep Purif Technol* **150**: 95-101 (2015).

36 Bradford MM, A rapid and sensitive method for the quantitation of microgram quantities of protein utilizing the principle of protein-dye binding. *Anal Biochem* **72**: 248-254 (1976).

37 Marella C, Muthukumarappan K and Metzger LE, Evaluation of commercially available, wide-pore ultrafiltration membranes for production of α–lactalbumin-enriched whey protein concentrate. *J Dairy Sci* **94**: 1165-1175 (2011).

38 Nigam MO, Bansal B and Chen XD, Fouling and cleaning of whey protein concentrate fouled ultrafiltration membranes. *Desalination* **218**: 313-322 (2008).

39 Juang R-S, Lin S-H and Peng L-C, Flux decline analysis in micellar-enhanced ultrafiltration of synthetic waste solutions for metal removal. *Chem Eng J* **161**: 19-26 (2010).

40 Mo H, Tay KG and Ng HY, Fouling of reverse osmosis membranes by protein (BSA): Effects of pH, calcium, magnesium, ionic strength and temperature. *J Membr Sci* **315**: 28-35 (2008).

41 Varzakas T, Tzia C, *Food Engineering Handbook, Food Process Engineering*, CRC Press, Taylor and Francis Group, USA (2015).

42 Hu K, Dickson JM, *Membrane Processing for Dairy Ingredient Separation*, Wiley Blackwell, Chicago, USA (2015).

43 Pasmore M, Todd P, Smith S, Baker D, Silverstein J, Coons D and Bowman C, Effects of ultrafiltration membrane surface properties on Pseudomonas aeruginosa biofilm initiation for the purpose of reducing biofouling. *J Membr Sci* **194**: 15-32 (2011).

44 Evans PJ, Bird MR, Pihlajamäki A and Nyström M, The influence of hydrophobicity, roughness and charge upon ultrafiltration membranes for black tea liquor clarification. *J Membr Sci* **313**: 250–262 (2008).

45 Ang W.S., Lee S., Elimelech M., 2006. Chemical and physical aspects of cleaning of organic-fouling reverse osmosis membranes. J. Membr. Sci. 272, 198-210.

46 Fox PF and McSweeney PLH, *Advanced Dairy Chemistry*, *Proteins*, vol. 1, Kluwer Academic/Plenum Publishers, New York (2003).

47 Edwards PB and Jameson GB, Chapter 7: Structure and stability of whey proteins in *Milk Proteins: From Expression to Food (Second Edition)*, ed by Taylor SL, Elsevier, London, pp 201-242 (2014).

48 Almécija MC, Martínez-Férez A, Guadix A, Páez MP and Guadix EM, Influence of the cleaning temperature on the permeability of ceramic membranes. *Desalination* **245**: 708-713 (2009).

49 Ang WS and Elimelech M, Protein (BSA) fouling of reverse osmosis membranes: implications for wastewater reclamation. *J Membr Sci* **296**: 83–92 (2007).

50 Ni Y, Wen L, Wang L, Dang Y, Zhou P and Liang L, Effect of temperature, calcium and protein concentration on aggregation of whey protein isolate: Formation of gel-like micro-particles. *Inter Dairy J* **51**: 8-15 (2015).

51 García-Ivars J, Iborra-Clar M-I, Alcaina-Miranda M-I, Mendoza-Roca J-A and Pastor-Alcañiz L, Treatment of table olive processing wastewaters using novel photomodified ultrafiltration membranes as first step for recovering phenolic compounds. *J Hazard Mat* **290**: 51-59 (2015).

52 Igbinigun E, Fenell Y, Malaisamy R, Jones KL and Morris V, Graphene oxide functionalized polyethersulfone membrane to reduce organic fouling. *J Membr Sci* **514**: 518-526 (2016).

53 Rahimpour A and Madaeni SS Improvement of performance and surface properties of nano-porous polyethersulfone (PES) membrane using hydrophilic monomers as additives in the casting solution. *J Membr Sci* **360**: 371-379 (2010).

54 Shang R, Vuong F, Hu J, Li S, Kemperman AJB, Nijmeijer K, Cornelissen ER, Heijman SGJ, Rietveld LC, Hydraulically irreversible fouling on ceramic MF/UF membranes: Comparison of fouling índices, foulant composition and irreversible pore narrowing. *Sep Purif Technol* **147**: 303-310 (2015).

55 Peyravi M, Rahimpour A, Jahanshahi M, Javadi A, Shockravi A, Tailoring the surface properties of PES ultrafiltration membranes to reduce the fouling resistance using synthesized hydrophilic copolymer. *Micropor Mesopor Mater* **160**: 114-125 (2012).

56 Razavi MA, Mortazavi A and Mousavi M, Dynamic modelling of milk ultrafiltration by artificial neural network. *J Membr Sci* **220**: 47-58 (2003).

57 Curcio S, Calabrò V, and Iorio G, Reduction and control of flux decline in cross-flow membrane processes modelled by artificial neural networks. *J Membr Sci* **286**: 125-132 (2006).

58 Robles, A, Ruano MV, Ribes J, Seco A and Ferrer J, Mathematical modelling of filtration in submerged anaerobic MBRs (SAnMBRs): Long-term validation. *J Membr Sci* **446:** 303-309 (2013).

59 Eleiwi F, Ghaffour N, Alsaadi AS, Francis L and Laleg-Kirati TM, Dynamic modeling and experimental validation for direct contact membrane distillation (DCMD) process. *Desalination* **384**: 1-11 (2016).

Table 1. Composition of the whey protein concentrates used in this work.

Whey component	WPC33 dry basis composition (w%)	WPC45 dry basis composition (w%)
Dry matter	95.16 ± 0.21	93.66 ± 0.95
Fat	6.06 ± 0.23	8.14 ± 0.20
Lactose	54.76 ± 0.49	38.27 ± 0.49
Total protein content	27.56 ± 0.39	40.74 ± 0.79
Ashes	10.56 ± 0.41	7.85 ± 0.07
Ca	1.03 ± 0.03	0.79 ± 0.06
Na	1.11 ± 0.06	1.21 ± 0.09
K	1.70 ± 0.01	1.42 ± 0.02

Table 2. Protein and calcium concentration in the feed solutions and protein rejection values for the membranes tested.

Feed solution	C_{prot} (g/L)	C_{Ca} (g/L)	Protein rejection (%)		
			5 kDa	15 kDa	30 kDa
BSA	10.00	0.00	99.72	99.76	99.75
BSA + $CaCl_2$	10.00	0.59	99.69	99.70	99.69
WPC45 22.2 g/L	9.05	0.18	99.98	99.79	99.93
WPC45 33.3 g/L	13.58	0.26	99.65	99.63	99.72
WPC45 44.4 g/L	18.11	0.35	99.59	99.55	99.67

Table 3. Values of the fitting parameters for the combined model.

Membrane	Feed solution	K_{CPB} (m^{-1})	K_{CF} ($\cdot 10^6$ s/m^2)	α_0 (dimensionless)	b (s^{-1})
5 kDa	BSA	32.715	2.681	0.481	0.154
	BSA + $CaCl_2$	53.873	9.005	0.509	0.149
	WPC45 22.2 g/L	81.995	22.060	0.769	0.156
	WPC45 33.3 g/L	82.114	25.320	0.834	0.173
	WPC45 44.4 g/L	83.247	30.330	0.892	0.270
15 kDa	BSA	26.306	2.135	0.255	0.183
	BSA + $CaCl_2$	37.517	5.136	0.447	0.159
	WPC45 22.2 g/L	45.356	8.863	0.593	0.153
	WPC45 33.3 g/L	67.590	16.770	0.737	0.159
	WPC45 44.4 g/L	86.709	27.880	0.822	0.157
30 kDa	BSA	16.326	0.695	0.099	0.174
	BSA + $CaCl_2$	20.992	1.370	0.313	0.263
	WPC45 22.2 g/L	40.010	4.040	0.700	0.565
	WPC45 33.3 g/L	40.480	4.871	0.846	0.150
	WPC45 44.4 g/L	40.600	5.778	0.951	0.145

Table 4. Fitting accuracy (in terms of R^2 and SD) for the combined model.

Feed solution	5 kDa		15 kDa		30 kDa	
	R^2	SD	R^2	SD	R^2	SD
BSA	0.982	0.011	0.993	0.008	0.983	0.008
BSA + $CaCl_2$	0.984	0.012	0.990	0.012	0.978	0.009
WPC45 22.2 g/L	0.985	0.012	0.975	0.024	0.986	0.008
WPC45 33.3 g/L	0.981	0.017	0.980	0.023	0.960	0.016
WPC45 44.4 g/L	0.985	0.019	0.981	0.023	0.985	0.009

Table 5. Mathematical equations for each model parameter and membrane used.

Membrane	Equation		
5 kDa	$\alpha_0 = 0.734 - 3.761\left(\frac{L^2}{g^2}\right)\cdot C_{Ca}^{\,2} - 0.003\left(\frac{L^2}{g^2}\right)\cdot C_{prot}^{\,2} + 0.229\left(\frac{L^2}{g^2}\right)\cdot C_{Ca}\cdot C_{prot}$	$R^2 = 0.999$	Eq. 5
	$K_{CPB} = 81.390\left(\frac{1}{m}\right) - 543.130\left(\frac{L^2}{m\cdot g^2}\right)\cdot C_{Ca}^{\,2} - 0.487\left(\frac{L^2}{m\cdot g^2}\right)\cdot C_{prot}^{\,2} + 35.911\left(\frac{L^2}{m\cdot g^2}\right)\cdot C_{Ca}\cdot C_{prot}$	$R^2 = 0.999$	Eq. 6
	$K_{CF} = 1.922\cdot 10^{7}\left(\frac{s}{m^2}\right) - 2.291\cdot 10^{8}\left(\frac{s\cdot L^2}{m^2\cdot g^2}\right)\cdot C_{Ca}^{\,2} - 1.654\cdot 10^{5}\left(\frac{s\cdot L^2}{m^2\cdot g^2}\right)\cdot C_{prot}^{\,2} + 1.471\cdot 10^{7}\left(\frac{s\cdot L^2}{m^2\cdot g^2}\right)\cdot C_{Ca}\cdot C_{prot}$	$R^2 = 0.999$	Eq. 7
15 kDa	$\alpha_0 = 0.524 - 3.831\left(\frac{L^2}{g^2}\right)\cdot C_{Ca}^{\,2} - 0.003\left(\frac{L^2}{g^2}\right)\cdot C_{prot}^{\,2} + 0.260\left(\frac{L^2}{g^2}\right)\cdot C_{Ca}\cdot C_{prot}$	$R^2 = 0.999$	Eq. 8
	$K_{CPB} = 29.129\left(\frac{1}{m}\right) - 201.286\left(\frac{L^2}{m\cdot g^2}\right)\cdot C_{Ca}^{\,2} + 13.401\left(\frac{L^2}{m\cdot g^2}\right)\cdot C_{Ca}\cdot C_{prot}$	$R^2 = 0.984$	Eq. 9
	$K_{CF} = 2.284\cdot 10^{6}\left(\frac{s}{m^2}\right) - 8.852\cdot 10^{7}\left(\frac{s\cdot L^2}{m^2\cdot g^2}\right)\cdot C_{Ca}^{\,2} + 5.753\cdot 10^{6}\left(\frac{s\cdot L^2}{m^2\cdot g^2}\right)\cdot C_{Ca}\cdot C_{prot}$	$R^2 = 0.999$	Eq. 10
30 kDa	$\alpha_0 = 0.634 - 7.255\left(\frac{L^2}{g^2}\right)\cdot C_{Ca}^{\,2} - 0.005\left(\frac{L^2}{g^2}\right)\cdot C_{prot}^{\,2} + 0.468\left(\frac{L^2}{g^2}\right)\cdot C_{Ca}\cdot C_{prot}$	$R^2 = 0.998$	Eq. 11
	$K_{CPB} = 39.900\left(\frac{1}{m}\right) - 286.023\left(\frac{L^2}{m\cdot g^2}\right)\cdot C_{Ca}^{\,2} - 0.236\left(\frac{L^2}{m\cdot g^2}\right)\cdot C_{prot}^{\,2} + 17.824\left(\frac{L^2}{m\cdot g^2}\right)\cdot C_{Ca}\cdot C_{prot}$	$R^2 = 0.999$	Eq. 12
	$K_{CF} = 3.505\cdot 10^{6}\left(\frac{s}{m^2}\right) - 4.226\cdot 10^{7}\left(\frac{s\cdot L^2}{m^2\cdot g^2}\right)\cdot C_{Ca}^{\,2} - 2.810\cdot 10^{4}\left(\frac{s\cdot L^2}{m^2\cdot g^2}\right)\cdot C_{prot}^{\,2} + 2.631\cdot 10^{6}\left(\frac{s\cdot L^2}{m^2\cdot g^2}\right)\cdot C_{Ca}\cdot C_{prot}$	$R^2 = 0.999$	Eq. 13

With α_0: limiting value of the pore blocking parameter, K_{CPB}: constant of the complete pore blocking model, K_{CF}: constant of the cake formation model, C_{Ca}: calcium concentration, C_{prot}: protein concentration.

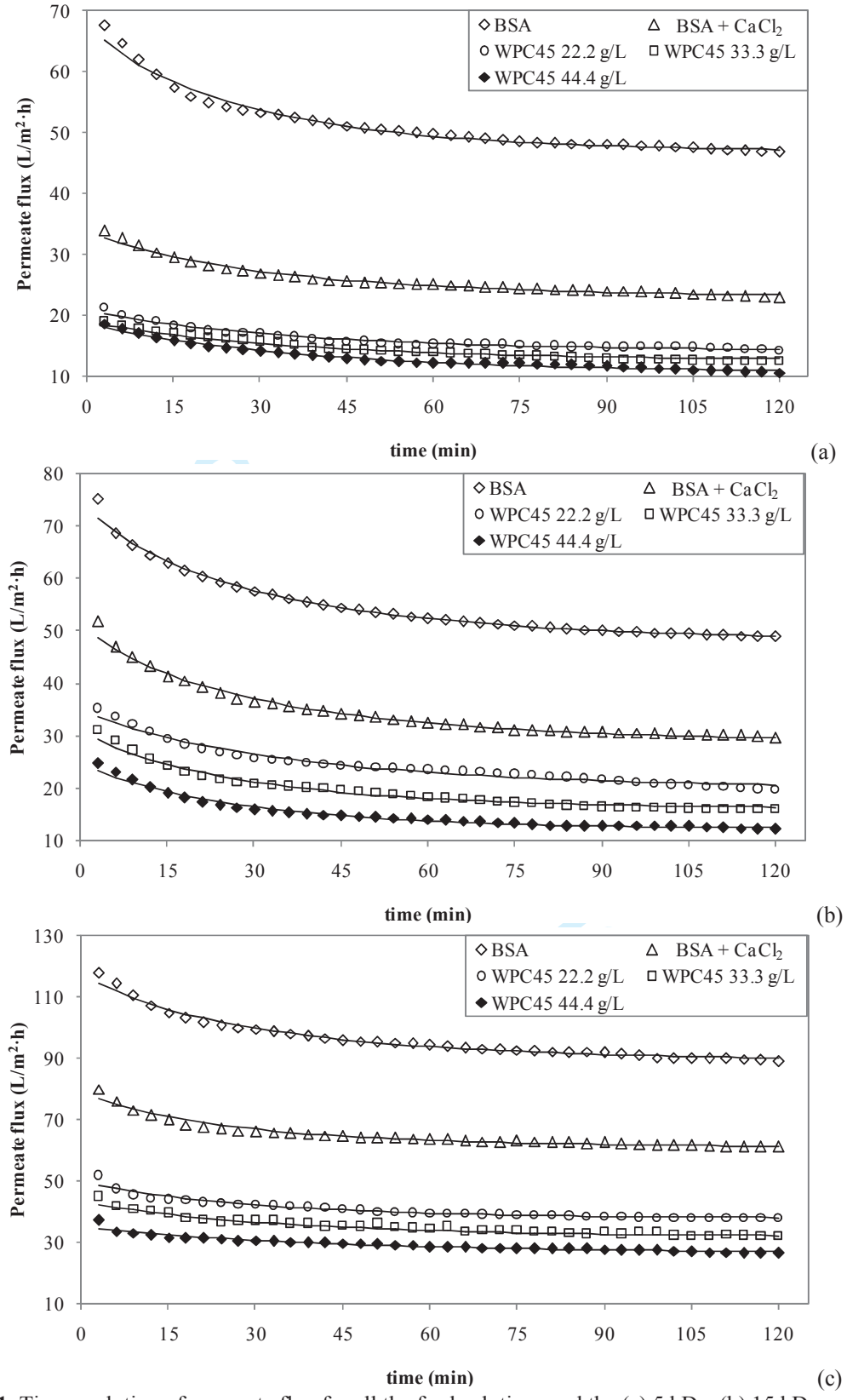

Fig. 1. Time evolution of permeate flux for all the feed solutions and the (a) 5 kDa, (b) 15 kDa and (c) 30 kDa membranes (combined model estimations: solid lines; experimental data: symbols).

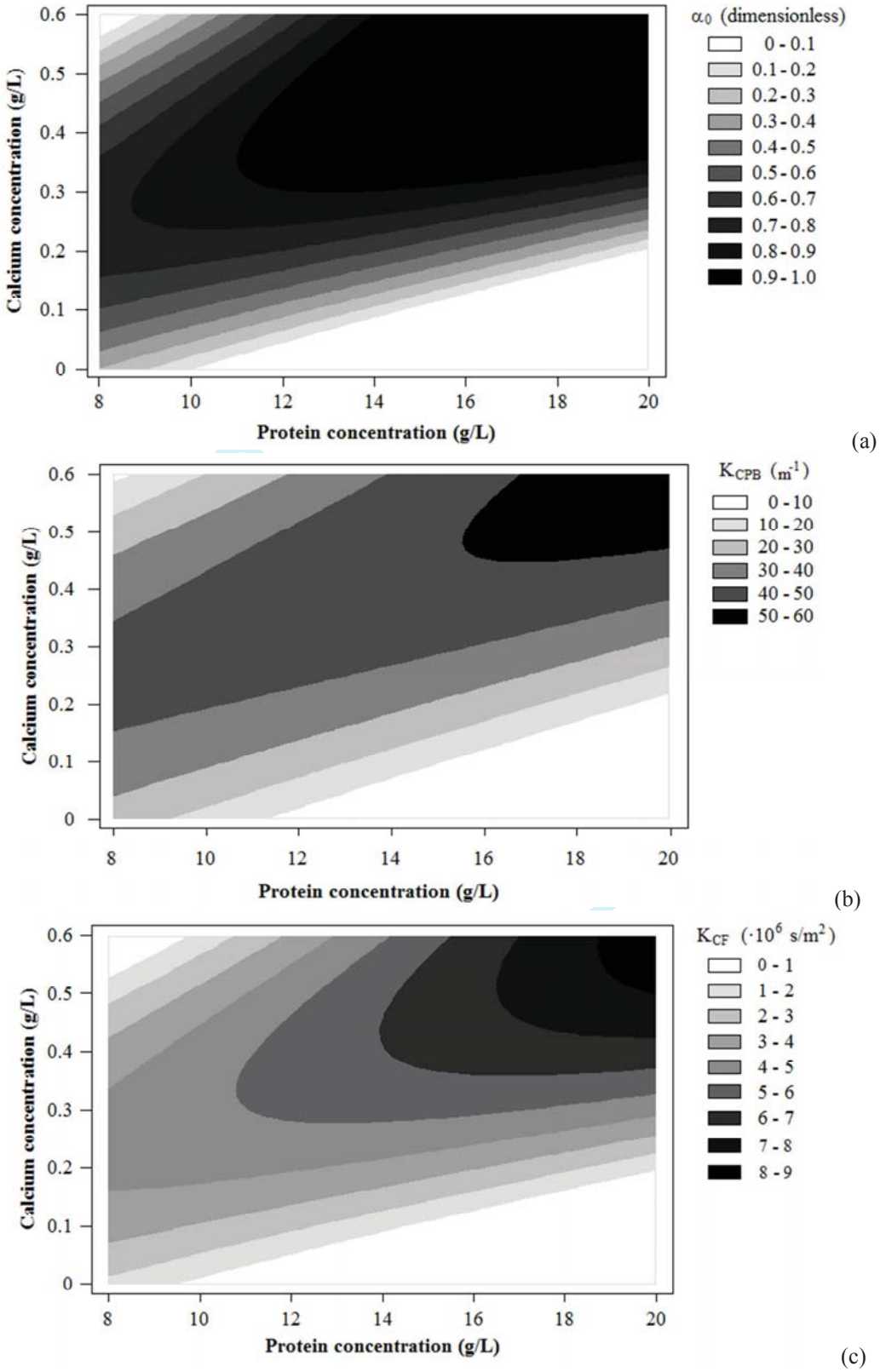

Fig. 2. Influence of calcium and protein concentration in the feed solution on the model parameters (a) α_0, (b) K_{CPB} and (c) K_{CF} for the 30 kDa membrane.

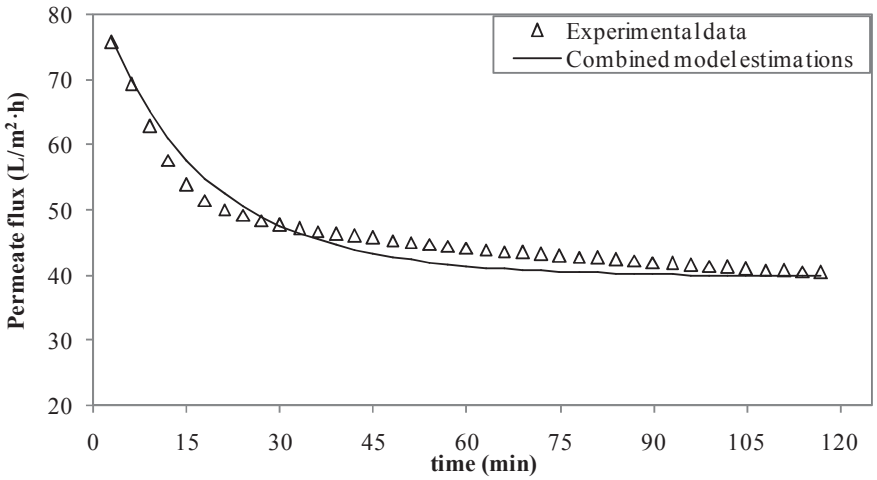

Fig. 3. Time evolution of permeate flux for WPC33 solutions at 30.3 g/L for the 30 kDa membrane (combined model estimations: solid lines; experimental data: symbols).